Break-up of the Larsen B Ice Shelf Triggered by Chain-Reaction Drainage of Supraglacial Lakes

Alison F. Banwell[1,2], Douglas R. MacAyeal[1] and Olga V. Sergienko[3]

[1]The Department of Geophysical Sciences, The University of Chicago, Chicago, IL, USA.

[2] Scott Polar Research Institute, University of Cambridge, Cambridge, UK.

[3]The Atmospheric and Oceanic Sciences Program, Princeton University, Princeton, NJ, USA.

The explosive disintegration of the Larsen B Ice Shelf poses two unresolved questions: What process (1) set a horizontal fracture spacing sufficiently small to pre-dispose the subsequent ice-shelf fragments to capsize, and (2) synchronized the widespread drainage of >2750 supraglacial meltwater lakes observed in the days prior to break-up? We answer both questions through analysis of the ice shelf's elastic-flexure response to the supraglacial lakes on the ice shelf prior to break-up. By expanding the previously articulated role of lakes beyond mere water-reservoirs supporting hydrofracture, we show that lake-induced flexural stresses produce a fracture network with appropriate horizontal spacing to induce capsize-driven break-up. The analysis of flexural stresses suggests that drainage of a single lake can cause neighboring lakes to drain, which, in turn, cause farther removed lakes to drain. Such self-stimulating behavior can account for the sudden, widespread appearance of a fracture system capable of driving explosive break-up.

1. Introduction

A number of studies have documented the explosive disintegration of the Larsen B Ice Shelf (LBIS) over a time period of just a few days in March 2002 [e.g., *Scambos et al.,* 2003; *Shepherd et al*., 2003; *Rignot et al.,* 2004; *Glasser and Scambos,* 2008]. However, two key questions remain unresolved. First, no previous study has suggested a mechanism that drove the ice shelf to separate into thousands of fragments possessing aspect ratios (horizontal length to ice thickness) that are less than the critical value (~0.6) necessary for capsize (and thus ice-shelf disintegration through capsize-liberated energy)

[*MacAyeal et al.,* 2003; 2011; *Burton et al.,* 2012]. Second, although multiple studies have documented both the emergence of >2750 supraglacial lakes during the decade prior to break-up [e.g., *Glasser and Scambos*, 2008] and their drainage, likely by hydrofracture [e.g., *Scambos et al.,* 2000; 2003; 2009], in the days leading up to the LBIS break-up, no previous study has explained the extraordinary synchronicity of lake drainage over such a short time period. These two unresolved questions, however, must be answered to fully understand the mechanisms which drove the break-up of the LBIS and to make predictions regarding the fate of other Antarctic ice shelves.

2. Ice-Shelf Flexural Response to Meltwater Loads

Flexure of an ice shelf subject to surface meltwater loads can be modeled using thin elastic (Kirchhoff) plate theory [e.g., *Kerr*, 1976; *Sergienko*, 2005; *MacAyeal and Sergienko*, 2013, *Sergienko* 2013]. When a lake fills (Figure 1a), the gravitational load depresses the ice shelf, and causes a flexure-induced uplift, or forebulge, to arise in a ring surrounding the lake. If the lake's horizontal span is smaller than a length-scale L ~1000 m, determined by flexural dynamics (see Methods 1 in the auxiliary material), as is the case for the majority of lakes mapped on the LBIS [*Glasser and Scambos*, 2008], the forebulge will be located at a distance of roughly $2L \approx 2$ km from the center of the lake (see Figure S1 in the auxiliary material). In the forebulge, tensile stress at the ice-shelf surface can initiate and promote fracture in the form of a ring-like surface rift [*Beltaos*, 2002], which surrounds the lake at a distance of ~2 km. This style of fracture occurs in many other geophysical settings, e.g., as is exemplified by the study of volcanic calderas and seamounts [*Lambeck and Nakiboglu*, 1980; *Williams and Zuber*, 1995]. Water, both present in lakes and flowing across the surrounding bare ice, will fill the fracture, enabling it to penetrate deeper [e.g. *van der Veen*, 1998; *Scambos et al.,* 2000]. In addition to the ring-type surface fracture, a fracture produced by tensile stress at the ice shelf base, immediately below the lake, would propagate upward in a radial, linear pattern [*Beltaos*, 2002] (Figure 1a).

The hydrostatic rebound of a drained lake will induce complementary fractures in the ice shelf that have similar geometry to those described above, but which originate on opposite surfaces of the ice shelf (Figure 1b). Under the assumption that the time-scale of lake drainage is very short compared to the Maxwell time [*Maxwell*, 1867], an elastic treatment of flexure stresses induced immediately following drainage is valid [*MacAyeal and Sergienko*, 2013]. However, as it takes several years for a lake to develop its size through filling/draining and/or refreezing of meltwater, there is a viscous component in the ice-shelf response as well [*Kerr*, 1976; *Beltaos*, 2002; *Sergienko*, 2005]. Additionally, as lake-bottom ablation will exceed the ablation of surrounding bare ice (as lake water has a lower albedo than the surrounding bare ice) [*Tedesco et al.,* 2012], a fraction of the ice shelf thickness is released as water accompanying the drainage of the original meltwater load (Figure 1b). The empty, often uplifted lake basins are called 'dolines' in analogy to sinkholes in karst terrain [*Bindschadler et al.,* 2002; *MacAyeal and Sergienko,* 2013]. They are often the deepest meltwater-derived features (>10 m) on an ice shelf, suggesting that, prior to drainage, a multi-year englacial water body existed within the ice shelf [*Bindschadler et al.,* 2002].

Cycling between filled and drained states over a period of several years suggests that the fracture patterns developed by meltwater loads and dolines (anti-loads) are likely to occur in tandem, such as is shown in Figure 1c. In this illustration, upward propagating fractures from the ice-shelf base meet downward propagating fractures from the ice-shelf surface leading to through-cutting rifts.

3. Fragmentation Length Scales of Ice Shelves

To show that that the lake/doline-induced fracture process described above could have fragmented the LBIS into pieces small enough to be capable of capsize [*MacAyeal et al.,* 2003], we compute the idealized fracture pattern across the LBIS using the exact analytic solution [*Kerr*, 1976; *Sergienko*, 2005; *MacAyeal and Sergienko*, 2013] for flexure of a thin elastic plate (Figure S1). For a full description of the solution, the elastic plate flexure equation it obeys, and the boundary conditions, refer to *Sergienko* [2005].

For each lake, we associate an azimuthally symmetric stress-field filling the surrounding area ($r>0$, where $r=0$ is the lake center) as if the lake were imbedded in an ice shelf of uniform thickness, $H=200$ m [*Sandhager et al.,* 2005], and of infinite extent. Figure S1 shows this stress-field, computed analytically for an example lake of 500 m radius and 1 m depth. In the following calculations, we assume that lakes are homogeneous in depth, *d* (to be described below), and choose a lake radius so that the area is equal to that of the real lake on the LBIS, and where the lake center is located as observed.

Replacement of the observed lakes (by *Glasser and Scambos* [2008], from February 2000) by disk-shaped lakes of constant depth with equal area as the observed lakes is justified when the radii of lakes on the LBIS (averaging ~170 m) are much smaller than the length-scale, *L* ~1000 m. When this is condition is satisfied, the numerical solution for an arbitrary shape/depth differs negligibly from the analytic solution for a uniform disk load (refer to Methods 2 in the auxiliary material for an illustration of this).

With this idealization, and with a distribution of lakes on the LBIS derived from observation of position and area [*Glasser and Scambos,* 2008], we compute the loci of ring-type fractures, by computing the radius of maximum tensile stress on the forebulge around lake centers. (We do not consider the radial, spoke-like, linear fractures centered on the lake's antipode [*Beltaos*, 2002], because we do not have a methodology for determining their orientation. If they were considered, the aspect ratio of ice-shelf fragments would be further reduced because there would be more fractures.) The presence or absence of the ring-type fracture surrounding any given lake will, of course, depend on whether the lake is deep enough for the stress field it creates to exceed the criterion necessary for fracture initiation. It would also depend on whether there is sufficient water in the area [*Sergienko and MacAyeal,* 2005] to support continued development of the fracture via the hydrofracture mechanism discussed by *Scambos et al.* [2000; 2003]. Thus, we simply assume that the required lake depth for ring-type fractures is met at the radius where maximum tensile stress is achieved.

Figure 2b depicts the fracture pattern using the observed lakes represented as disk loads. The areas divided by the intersecting rings represent the ice-shelf fragments that became separate icebergs at the outset of the LBIS break-up. To determine which fragments in Figure 2b would likely capsize and disintegrate, we estimated the axis of capsize (horizontal axis around which the ice fragment would rotate by 90°) and compared the maximum width perpendicular to this axis with the critical length scale, $\square_c H$ (m), where H=200 m is ice thickness, and were $\square_c$=0.6 is the critical aspect ratio necessary for iceberg capsize (and subsequent break-up), as described in *Burton et al.* [2012]. If the maximum width was less than this dimension, the ice fragment was deemed capsizable. As Figure 2c shows, ~60% of the original ice-shelf area is broken into fragments with an aspect ratio <0.6. We depict the capsized fragments in Figure 2c as blue ice mélange, assuming that they are obliterated during capsize. Comparison of the immediate, post-collapse imagery of the LBIS [*MacAyeal et al.,* 2003] with the depiction of capsized fragments in Figure 2c suggests that the process we propose is indeed potentially responsible for fragmenting the ice shelf in a manner sufficient to cause widespread capsize.

4. Self-Catalyzed Lake Drainage

We next show that lake drainage—the event that leads to lake-induced flexure fractures—can be self-catalyzed and self-sustaining, and can cooperatively occur across widely varying flow and stress regimes of the LBIS. To demonstrate this, we again use the same analytic solution, idealizations, and lake distribution on the LBIS as described in Section 3.

As the elastic flexure of an ice shelf with uniform thickness is a linear process [*Sergienko*, 2013], the linear superposition principle is applicable, and the flexural effect of multiple drained lakes is a sum of the flexural effects of individual lakes. However, for the purpose of demonstrating chain-reaction lake drainage, we need only to consider individual, not superimposed, lake-flexure solutions. This is because, with the assumption that the ice has visco-elastically relaxed in response to the emplacement of a mass of many lakes, if any one single lake (known as a ‘starter lake’) suddenly changes (either by taking on, or giving off, mass), it will have an immediate local stress-inducing effect on the stress regime of the surrounding ice shelf. As the starter lake causes surrounding lakes to drain, a ‘propagating front’ of lake drainage develops, with each stage of lake drainage events occurring further away from the position of the starter lake. This drainage front is always moving outward from the place where interference between individual lake drainage events could exist (but would have no relevance to whether new lakes would drain, as they are in a zone where all the lakes have already drained) into undisturbed, visco-elastically relaxed, ice.

Therefore, considering each lake separately, we assume that its drainage removes the equivalent load of 5 m of fresh water (density 1000 kg m^{-3}). This load represents the combination of enhanced lake-bottom ablation relative to surrounding bare ice, as well as the removal of water that filled the lake, assuming that the elastic response to the water load had visco-elastically relaxed [*Beltaos*, 2002; *Sergienko*, 2005] over the preceding portion of the melt season leading up to the event. With this reference load, we compute the von-Mises stress (T_{vM}) induced by the drainage of one lake at the center of every other lake on the ice shelf. Here, T_{vM} is defined to be:

$$T_{vM} = (T_{rr}^2 + T_{\theta\theta}^2 - T_{rr}T_{\theta\theta}^{1/2}. \qquad (1),$$

where T_{rr} and $T_{\theta\theta}$ are the radial and azimuthal stresses, respectively, and where r is the radial coordinate and θ is the azimuthal coordinate for a cylindrical reference system with origin at the center of the lake. Where the von-Mises stress exceeds the critical value 70 kPa (as recommended by *Albrecht and Levermann* [2012]), we assume that a fracture will develop at the bottom of the surrounding lake that can potentially drain it.

Figure 3a shows the single lake (labeled 'starter lake') that was found to stimulate drainage of the greatest number of surrounding lakes. With the chosen T_{vM} fracture criterion of 70 kPa, the number of lakes drained by the starter lake was 63. For this starter lake, we also considered the cascade of indirect influence that accounts for subsequent relationships between directly drained lakes and other lakes not initially drained by the starter lake. This yielded 10 stages of indirect influence and caused 227 lakes on the ice shelf to drain (~8% of the total number of lakes, 2758, reported by *Glasser and Scambos* [2008]). This number increased to 626 over 14 stages of indirect influence, or to ~23% of the total number of lakes, when the T_{vM} fracture criterion is reduced to 35 kPa (Figure 3b).

The ultimate implication of the interrelated causality of lake drainage is that a self-stimulating chain-reaction of lake drainage can develop across the LBIS. We regard this as a plausible explanation for the abrupt, widespread drainage of lakes observed in the days prior to the LBIS break-up [*Scambos et al.,* 2003]. We also argue that this process is sufficiently independent of other ice-shelf variables (e.g., the stress regime that drives glaciological ice-flow, due to the significantly slower time scale of viscous deformation compared to the disintegration) as to be plausible as the mechanism that kindled the explosive break-up.

As previously mentioned, in the computations made to create Figure 3, we assumed a constant depth of 5 m for all the lakes. This is a plausible depth for observed dolines [*Bindschadler et al.,* 2002; *Tedesco et al.,* 2012], but is at the upper limit of lake depths observed using February 2000 Landsat imagery [*Banwell et al*., in press], acquired 2 years prior to the collapse, where mean lake depths were ~1 m. To provide an indication of the sensitivity of fracture initiation to lake depth, we compute the depth needed in a circular lake of radius 500 m necessary to produce T_{vM} in excess of 70 kPa at any given distance r from the lake center. The result is shown in Figure 4. To fracture a 200 m thick ice shelf (comparable to the LBIS thickness when it broke-up) at a given distance r from the center of the lake, the lake must have the depth corresponding to those values depicted by the red curve in Figure 4. Thus, a lake has to be at least 1 m deep for the flexure-induced stress at the ice-shelf surface to exceed the fracture criterion (70 kPa) for a radial-type fracture to initiate at the lake center, and the lake has to be at least ~3.5 m deep for the ring-type fracture to occur at ~1700 m from the lake center. Reducing the critical stress criterion by half (to 35 kPa) necessitates only ~2 m depth to create the ring-type fracture along the forebulge.

Figure 4 also shows the effect of thinning the ice-shelf by 25 m. Such thinning could have occurred due to increased basal melting prior to the break-up of LBIS [*Shepherd et al*., 2003; *Vieli et al.,* 2007]). This suggests that there were two avenues by which warming and enhanced ablation of the LBIS could have pushed it towards conditions primed for break-up. Surface warming would induce continued lake deepening, whereas ocean warming (and consequent ice-shelf thinning) would continue to reduce the critical lake depth necessary to produce ring-type fractures. In addition, increased basal melting leads to substantial cooling of the ice shelf interior [*Sergienko et al.,* 2013], making it more susceptible to fracturing due to the fact that fractures in cold ice are less likely to be arrested than in warm ice [e.g., *Liu and Miller*, 1979].

5. Conclusions and Perspectives

We have shown that supraglacial lakes (and drained lakes) are mass loads (or deficits) that create flexure stresses on ice shelves. The estimated flexural tensile stresses are sufficiently large to initiate and propagate fractures, and the spacing of the fractures is determined by the spatial distribution and depths of lakes. We show that the spacing of these fractures caused a large proportion of the LBIS fragments to have aspect ratios that were unstable to capsize. We also show that the filling or drainage of a single 'starter lake' can produce multiple fractures that are able to drain hundreds of surrounding lakes through a chain-reaction process. Thus, we argue that this chain-reaction would contribute to the abruptness of the explosive disintegration of the LBIS.

The ultimate proof for the hypotheses we have proposed here depends on observations. If current warming trends prevail, lake-induced break-up may threaten other Antarctic ice shelves. We suggest that future research should consider whether the development of a large number of supraglacial lakes constitutes the essential tipping point, which, once reached, predetermines an ice shelf to break-up.

Acknowledgements

This research is supported by the U.S. National Science Foundation under grant GEOP/ANT – 0944248 awarded to D.R.M and grants ANT-0838811 and ARC-0934534 awarded to O.V.S. The authors acknowledge the valuable discussion and assistance of Neil Arnold, Neil Glasser, Martamaria Caballero and Ian Willis. Neil Glasser generously provided digitized outlines of lakes and dolines on the LBIS used in this study. Finally, the authors thank Anders Levermann, one anonymous reviewer, and the editor, Julienne Stroeve, for their valuable comments regarding our initial manuscript.

References

Albrecht, T., and A. Levermann (2012), Fracture field for large-scale ice dynamics. *J. Glaciol.,* 58(207), 165-176.

Banwell, A. F., M. Caballero, N. S. Arnold, N. F. Glasser, L. M. Cathles, and D. MacAyeal (in press), Supraglacial lakes on the Larsen B Ice Shelf, Antarctica, and the Paakitsoq Region, Greenland: a comparative study. *Ann. of Glaciol.,* 53(66), doi: 10.3189/2013AoG66A049

Beltaos, S. (2002), Collapse of floating ice covers under vertical loads: test data vs. theory. *Cold Reg. Sci. and Tech.*, 34, 191-207.

Bindschadler, R., T. A. Scambos, H. Rott, P. Skvarka, and P. Vornberger (2002), Ice dolines on Larsen Ice Shelf, Antarctica. *Ann. Glaciol.,* 34, 283-290.

Burton, J. C., J. M. Amundson, D. S. Abbot, A. Boghosian, L. M. Cathles, S. Correa-Legisos, K. N. Darnell, N. Guttenberg, D. M. Holland, and D. R. MacAyeal (2012), Laboratory investigations of iceberg capsize dynamics, energy dissipation and tsunamigenesis, *J. Geophys. Res.,* 117, F01007, doi:10.1029/2011JF002055.

Glasser, N. F. and T. A. Scambos (2008), A structural glaciological analysis of the 2002 Larsen Ice Shelf collapse. *J. Glaciol.,* 54(184), 3 -16.

Kerr, A. D. (1976), The bearing capacity of floating ice plates subjected to static or quasi-static loads. *J. Glaciol.,* 17(76), 229-268.

Lambeck. K., and S. M. Nakiboglu (1980), Seamount loading and stress in the ocean lithosphere. *J. Geophys. Res.* 85(B11), 6403-6418.

Liu H. W., and K. J. Miller (1979). Fracture toughness of fresh water ice . *J. Glaciol.,* 22(86), 135-143.

MacAyeal, D. R., T. A. Scambos, C. L. Hulbe, and M. A. Fahnestock (2003), Catastrophic ice-shelf break-up by an ice-shelf-fragment-capsize mechanism. *J. Glaciol.,* 49(164), 22-36.

MacAyeal, D. R., D. S. Abbot, and O. V. Sergienko (2011), Iceberg capsize tsunamigenesis. *Ann. Glaciol*., 52(58), 51-56.

MacAyeal, D. R., and O. V. Sergienko (2013), Flexural dynamics of melting ice shelves. *Ann. Glaciol*., 54(63), 1 – 10, doi: 10.3189AoG63A256.

Maxwell, J.C. (1867), On the dynamical theory of gases. *Phil. Trans. R. Soc. Lond.,* 157, 49–88.

Rignot, E., G. Casassa, P. Gogineni, W. Krabill, A. Rivera, and R Thomas (2004), Accelerated ice discharge from the Antarctic Peninsula following collapse of Larsen B ice shelf. *Geophys. Res. Lett.,* 31 (L18401), doi: 10.1029/2004GL020679.

Sandhager, H., W. Rack, and D. Jansen (2005), Model investigations of Larsen B Ice Shelf dynamics prior to the breakup. *FRISP Rep.* 16, 5–12

Scambos, T. A., C. Hulbe, M. Fahnestock, and J. Bohlander (2000), The link between climate warming and brea-up of ice shelves in the Antarctic Peninsula. *J. Glaciol.,* 46(154), 516-530.

Scambos, T. A., C. Hulbe, and M. A. Fahnestock (2003), M. A. Climate-induced ice shelf disintegration in the Antarctic Peninsula. In Domack, E. W., et al., eds. Antarctic Peninsula climate variability: a historical and paleoenvironmental perspective. Washington, DC, American Geophysical Union, 79-92 (Antarctic Research Series, 79), doi: 10.1029/AR079p0079.

Scambos, T., H. A. Fricker, C. C. Liu, J. Bohlander, J. Fastook, A. Sargent, R. Massom, and A. M. Wu (2009), Ice shelf disintegration by plate bending and hydro-fracture: Satellite observations and model results of the 2008 Wilkins ice shelf break-ups. *Earth Panet. Sci. Lett.,* 280(1-4), 51-60, http://dx.doi.org/10.1016/j.epsl.2008.12.027.

Sergienko, O. V. (2005), Surface melting of ice shelves and icebergs. PhD Thesis, University of Chicago, pp 128.

Sergienko O. and D. R. MacAyeal (2005). Surface melting on Larsen Ice Shelf, Antarctica. *Ann. Glaciol*., 40, 215-218.

Sergienko O.V., D. N. Goldberg and C. M. Little (2013), Alternative ice-shelf equilibriums determined by ocean environment. *J. Geophys. Res.,* 118, 970-981, doi:10.1002/jgrf.20054.

Sergienko O. V. (2013), Normal modes of a coupled ice-shelf/sub-ice-shelf cavity system. *J. Glaciol*., 59(213), 76-80, doi:10.3189/2013JoG12J096

Shepherd, A., D. Wingham, T. Payne, and P. Skvarca (2003), Larsen ice shelf has progressively thinned. *Science*, 302, 856-859, DOI: 10.1126/science.1089768.

Tedesco, M., M. Lüthje, K. Steffen, N. Steiner, X. Fettweis, I. Willis, N. Bayou, and A. Banwell (2012). Measurement and modeling of ablation of the bottom of supraglacial lakes in western Greenland. *Geophys. Res. Lett.,* 39, L02502, doi:10.1029/2011GL049882.

van der Veen, C. J. (1998), Fracture mechanics approach to penetration of surface crevasses on glaciers. *Cold Reg. Sci. and Tech*, 27, 31-47, doi: 10.1016/S0165-232X(97)00022-0

Vieli, A., A. J. Payne, A. Shepherd, and Z. Du (2007), Causes of pre-collapse changes of the Larsen B ice shelf: Numerical modelling and assimilation of satellite observations, *Earth Planet. Sci. Lett.,* 259, 297-306, doi:10.1016/j.epsl.2007.04.050.

Williams, K. K., and M. T. Zuber (1995), An experimental study of incremental surface loading of an elastic plate: application to volcano tectonics. *Geophys. Res. Lett.,* 22(15), 1981-1984, doi:10.1029/95GL02009.

Figures:

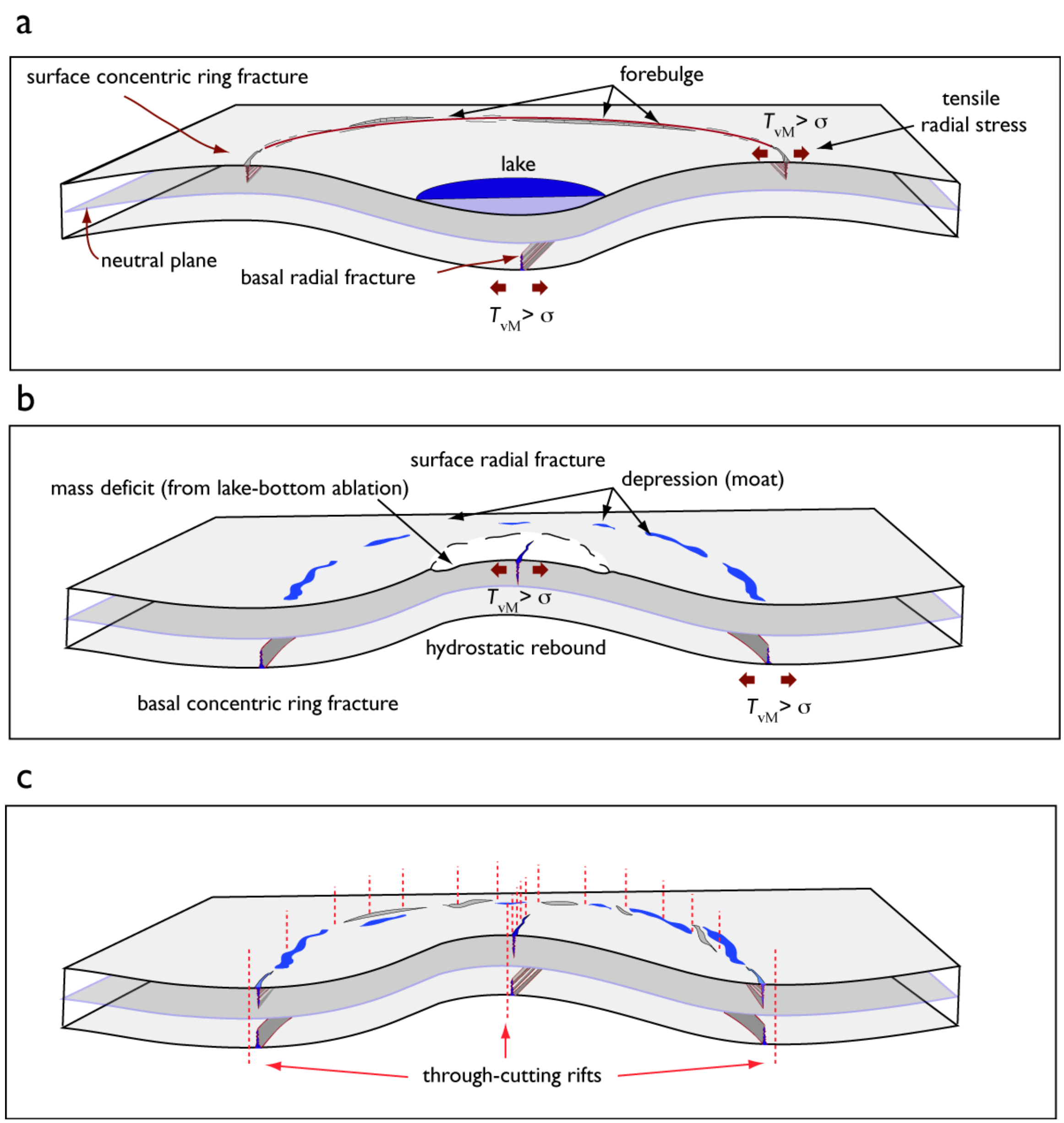

Figure 1. Schematic view of stress regime, flexure and fracture patterns associated with loaded (filled) and unloaded (drained) supraglacial lakes on ice shelves. a) As water fills an idealized circular depression, the accumulated mass creates a depression that induces an upward-deflected forebulge at a radial distance of ~2L. Downward propagating, ring-type fractures form in the forebulge at the ice-shelf surface. At the ice-shelf base, tension with upward radial propagating fractures form at the antipode of the lake. The neutral plane, where flexure stresses are zero and across which flexure stresses vary linearly to maximum amplitude at the surface and base of the ice shelf, is identified. b) When a lake

drains, hydrostatic rebound causes tensile stress to be induced in an inverted forebulge (surface moat). It is here that upward-propagating ring-type fractures are likely to form. The drained lake is also missing some original ice-shelf mass due to enhanced lake-bottom ablation. At the ice-shelf surface, tension with downward radial propagating fractures form at the antipode of the lake. c) Fractures introduced by repeated filling and draining of lakes over a number of years can potentially yield a mixed-mode fracture pattern, consisting of ring-type fractures surrounding the lake, and radial-type fractures below the lake depression.

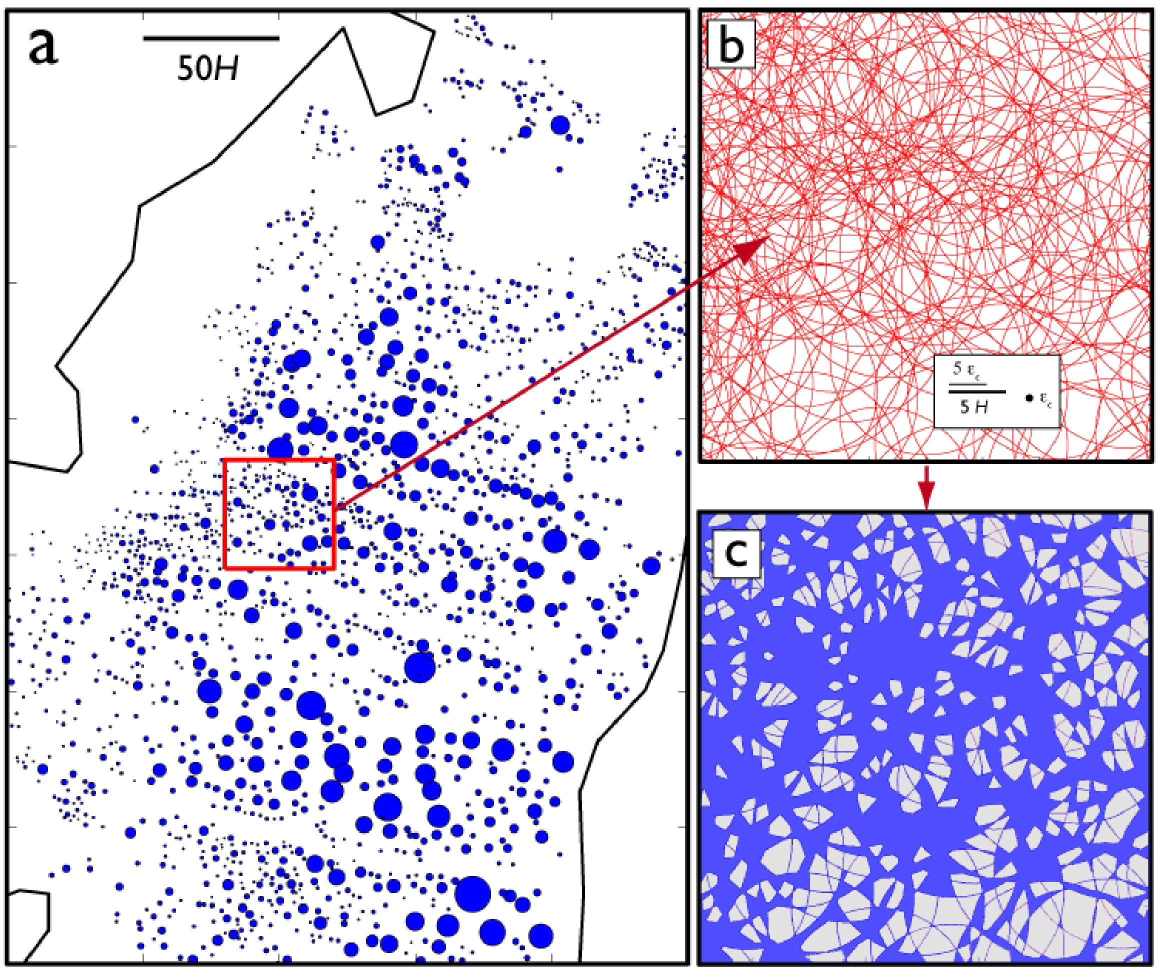

Figure 2. Break-up patterns associated with lake-induced flexure fractures (ring-type only) on the LBIS. a) Region map of the LBIS with observed lakes [*Glasser and Scambos,* 2008] represented as circles of equal area. The red box indicates the areas

represented in (b, c). b) Circles representing the loci of maximum von-Mises stress surrounding lakes located in the boxed region of the LBIS map shown in (a). These circles depict the ring-type fracture pattern that would be induced by lake filling or draining. c) Post-collapse ice-shelf fragment assemblage of the region shown in (b) assuming that fragments, where one of their two horizontal spans is less than the critical aspect ratio, $\square_c$ ~0.6, will capsize and become obliterated. Fragments that do not capsize are colored grey. Fragments that are capsized and assumed obliterated are replaced with blue mélange (colored blue).

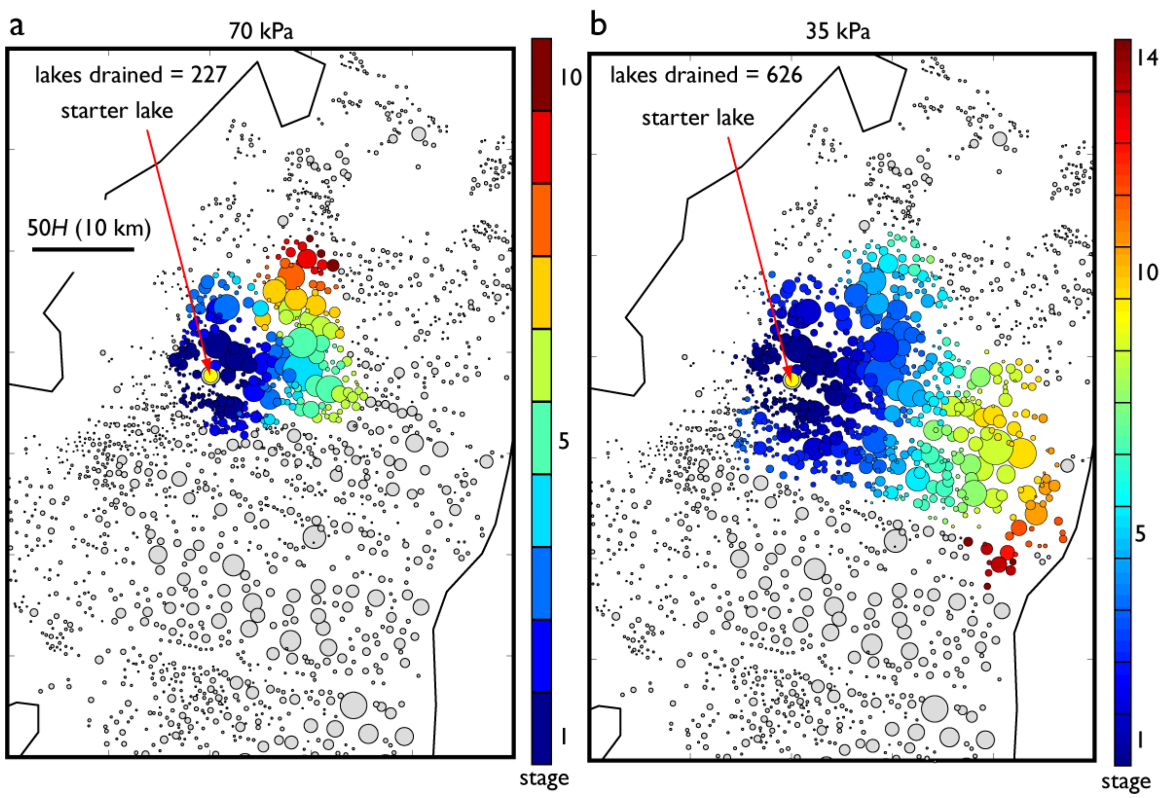

Figure 3. Chain-reaction drainage of supraglacial lakes. a) Observed lakes [*Glasser and Scambos*, 2008] are represented by circular disks of equal area and constant depth (5 m). The lake found to trigger the drainage of the most neighboring lakes is labeled 'starter lake'. Colored surrounding lakes indicate those that are induced to drain either directly by the starter lake's effect on flexure stresses (stage = 1) or indirectly by lakes which are drained at an earlier stage (stage = 2, …, 10). The color of the lake indicates its stage according to the color bar. When the fracture criterion of 70 kPa is evaluated at each

lake's center, a total of 227 lakes are triggered to drain by the starter lake (either directly or indirectly). The radii of colored lakes is drawn at twice the scale to promote visibility. The radii of gray shaded lakes, which are not drained as a result of the chain reaction, are drawn at true scale. b) As in (a), but with the fracture criterion reduced to 35 kPa. In this case, a total of 626 lakes are triggered to drain by the starter lake either directly (stage = 1), or indirectly (stage = 2, …, 14).

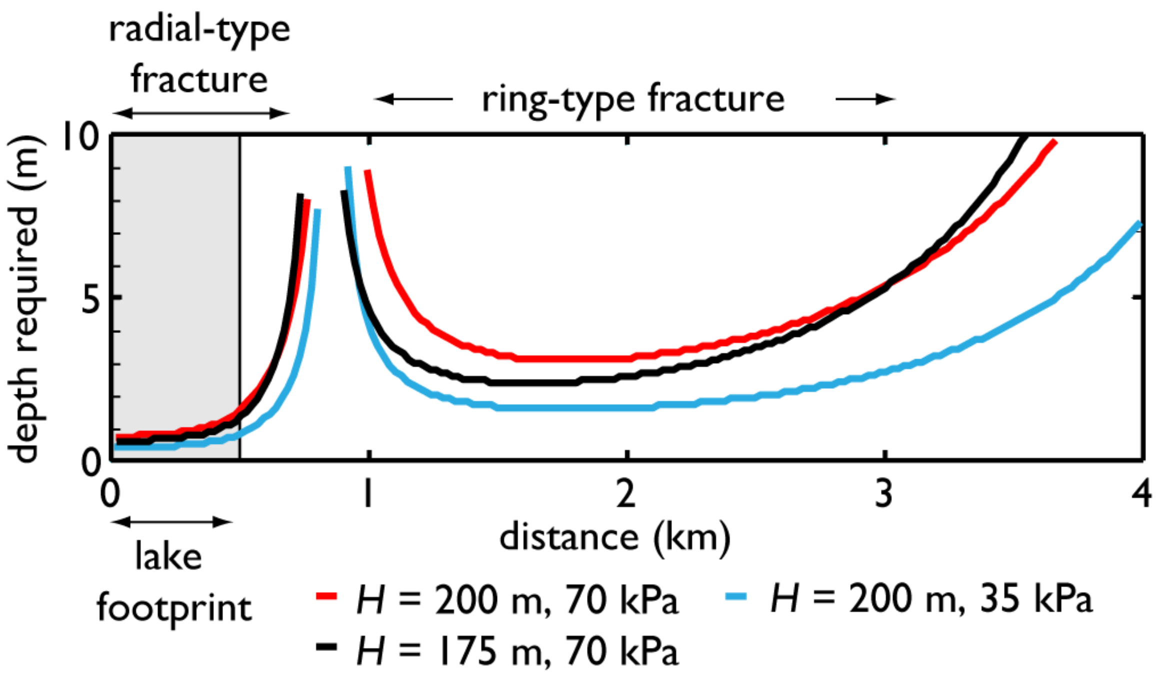

Figure 4. Critical lake depth required to induce fracture at the ice-shelf surface (ring-type fractures) or base (radial-type fractures) at a given distance (km), *r*, from the center of a circular lake with a 500 m radius assuming constant lake depth (m). For an ice-shelf thickness (*H*) of 200 m, the blue lines represent critical lake depth for a fracture criterion of 35 kPa, and the red lines represent critical lake depth for a fracture criterion of 70 kPa. The black lines represent critical lake depth if ice-shelf thickness is reduced by 25 m to *H* = 175 m. The footprint of the lake (*r* < 500 m) is shaded.

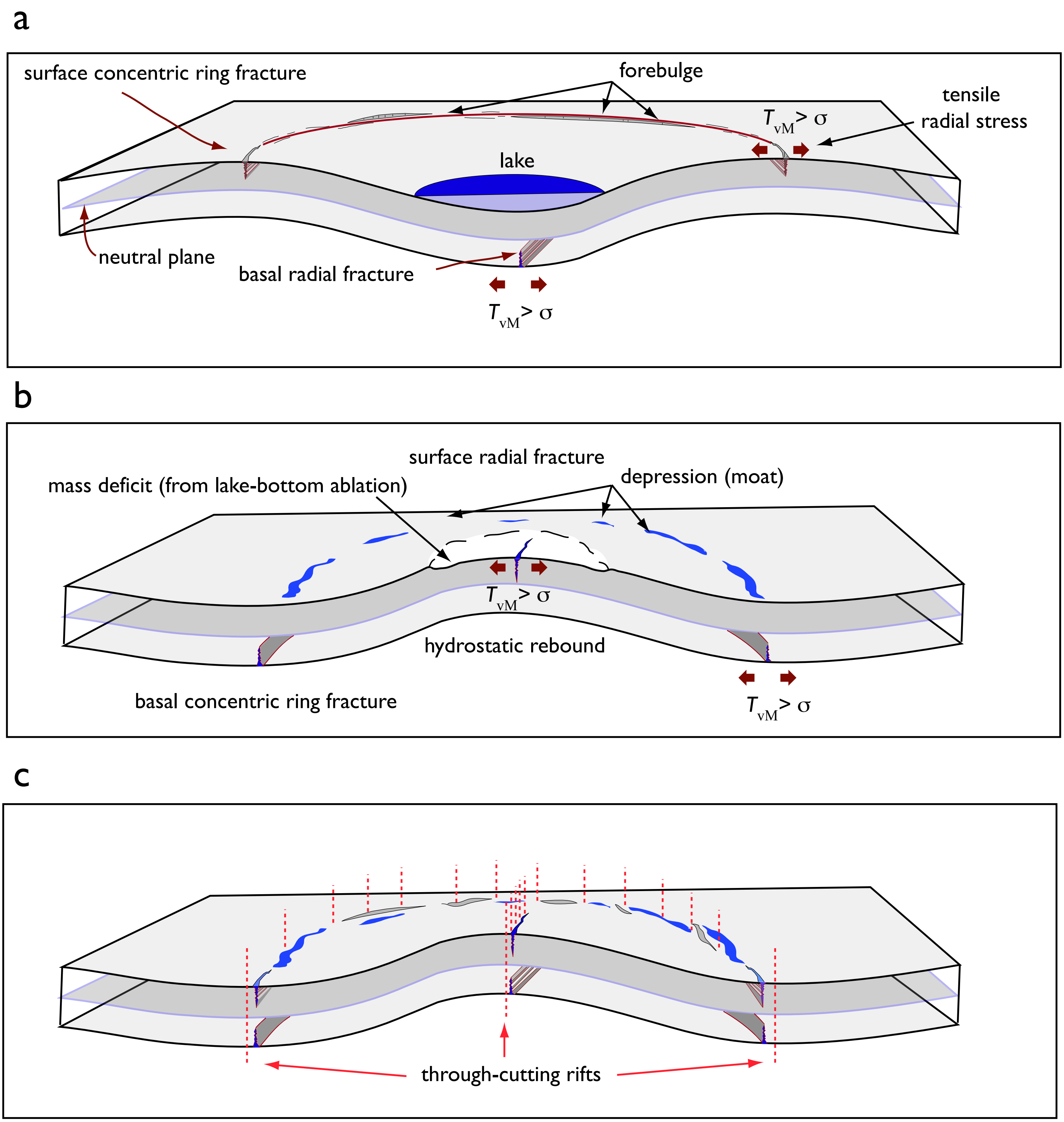
a
surface concentric ring fracture
forebulge
tensile
radial stress
$T_{vM} > \sigma$
lake
neutral plane
basal radial fracture
$T_{vM} > \sigma$
b
surface radial fracture
mass deficit (from lake-bottom ablation)
depression (moat)
$T_{vM} > \sigma$
hydrostatic rebound
basal concentric ring fracture
$T_{vM} > \sigma$
c
through-cutting rifts

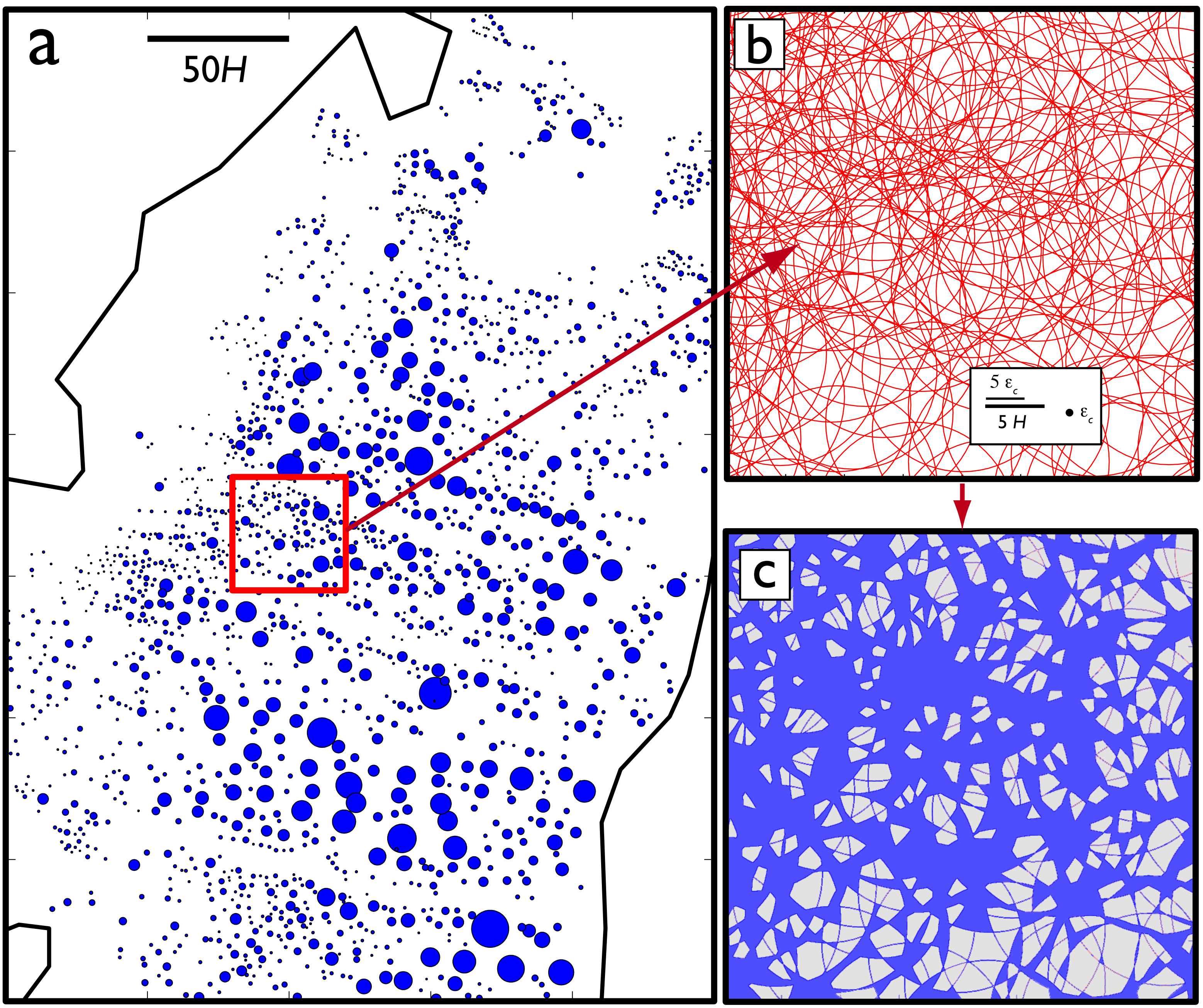
a
50H
b
5 ε_c
5 H
ε_c
c

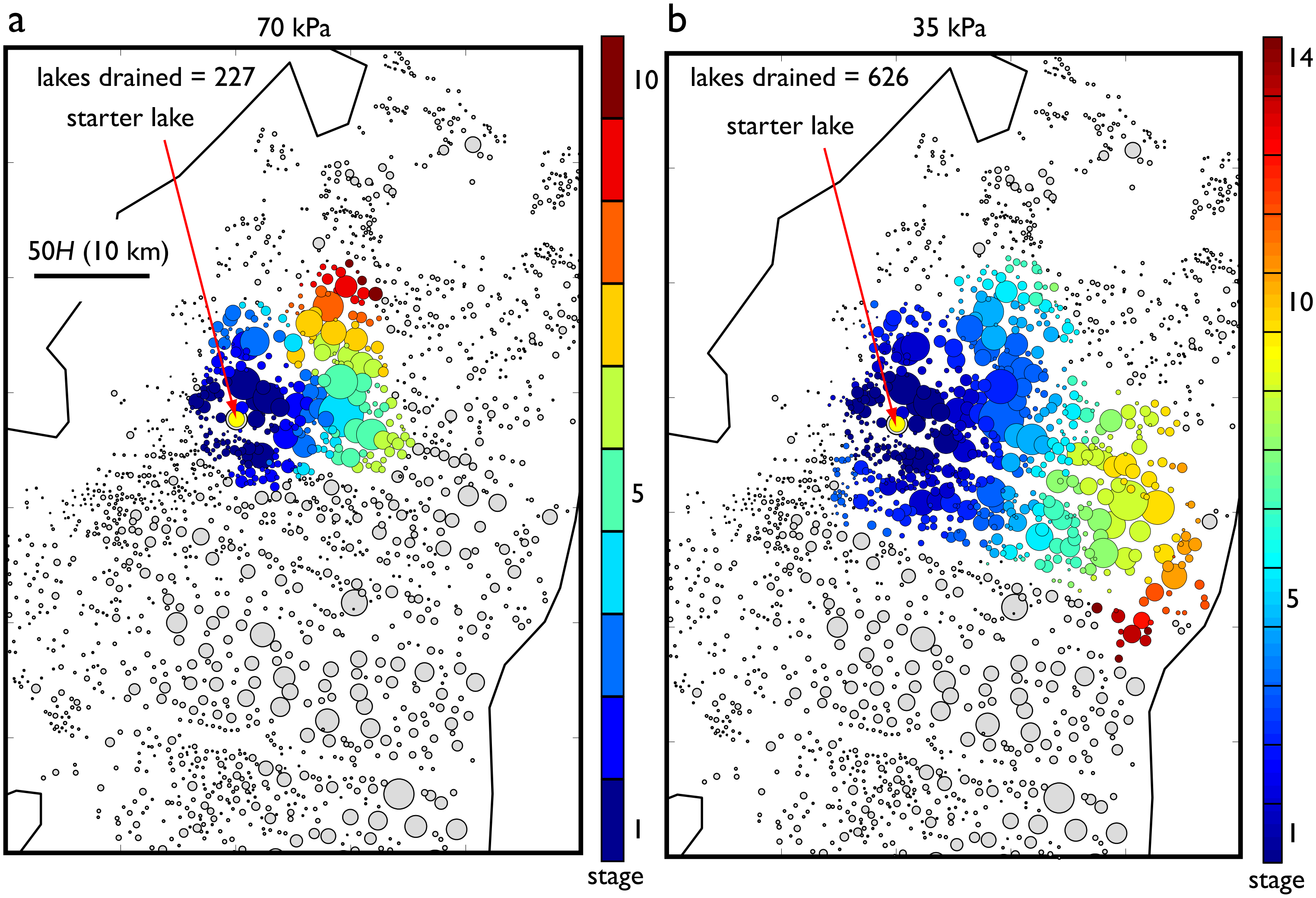

a
70 kPa
lakes drained = 227
starter lake
50H (10 km)
10
5
1
stage
b
35 kPa
lakes drained = 626
starter lake
14
10
5
1
stage

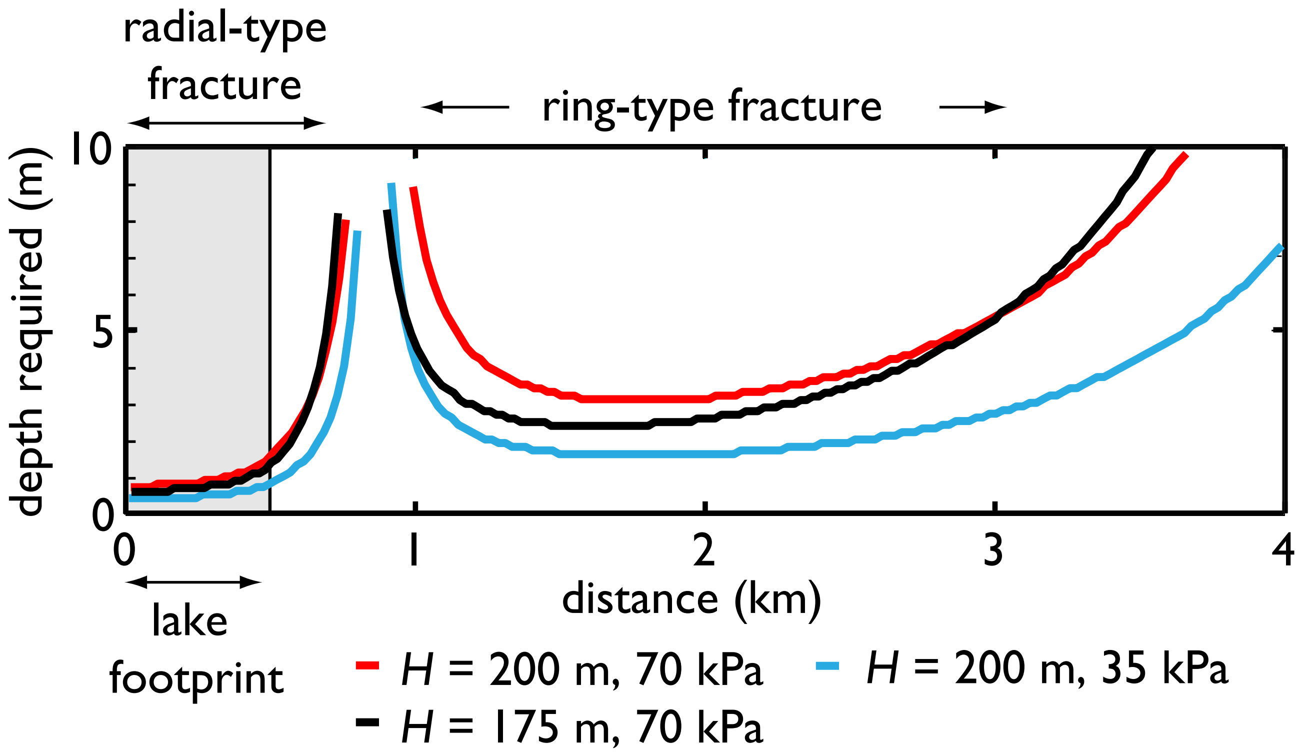
radial-type
fracture
ring-type fracture
depth required (m)
10
5
0
0
1
2
3
4
distance (km)
lake
footprint
H = 200 m, 70 kPa
H = 200 m, 35 kPa
H = 175 m, 70 kPa